

# Cervical Spine Range of Motion Measurement Utilizing Image Analysis

Kana Matsuo<sup>1</sup><sup>a</sup>, Koji Fujita<sup>2</sup><sup>b</sup>, Takafumi Koyama<sup>3</sup><sup>c</sup>, Shingo Morishita<sup>3</sup><sup>d</sup> and Yuta Sugiura<sup>1</sup><sup>e</sup>

<sup>1</sup>Department of Information and Computer Science, Keio University, Kanagawa, Japan

<sup>2</sup>Department of Functional Joint Anatomy, Tokyo Medical and Dental University, Tokyo, Japan

<sup>3</sup>Department of Orthopedic and Spinal Surgery, Tokyo Medical and Dental University, Tokyo, Japan

**Keywords:** Measurement System, Deep Learning, Cervical Spine, Range of Motion.

**Abstract:** Diseases of the cervical spine often cause more serious impediments to daily activities than diseases of other parts of the body, and thus require prompt and accurate diagnosis. One of the indicators used for diagnosing cervical spine diseases is measurements of the range of motion (RoM) angle. However, the main measurement method is manual, which creates a burden on physicians. In this work, we investigate the possibility of measuring the RoM angle of the cervical spine from cervical X-ray images by using Mask R-CNN and image processing. The results of measuring the RoM angle with the proposed cervical spine motion angle measurement system showed that the mean error from the true value was 3.5 degrees and the standard deviation was 2.8 degrees. Moreover, the standard deviation of the specialist measurements used for comparison was 2.9 degrees, while that of the proposed system was just 0 degrees, indicating that there was no variation in the measurements of the proposed system.

## 1 INTRODUCTION

In the medical field, many diagnostic imaging tests (e.g., those on X-ray images) are performed, but it is inconvenient for physicians to examine a large number of images and it takes away from the time they could be spending on medical treatment. In addition, at night, when only a small number of physicians are on duty, they may be asked to perform diagnostic imaging in areas in which they do not specialize. For this reason, there has been extensive research in recent years on automatic image diagnosis using artificial intelligence (AI).

The cervical spine is one of the areas on which many imaging studies have been focused, especially in orthopedics. When the degeneration of the cervical spine progresses due to aging, it causes cervical pain as well as neurological diseases such as myelopathy and radiculopathy. When myelopathy worsens, it causes dyskinesia of the fingers and gait, resulting in serious obstacle in daily life, so a prompt and accurate diagnosis is required.

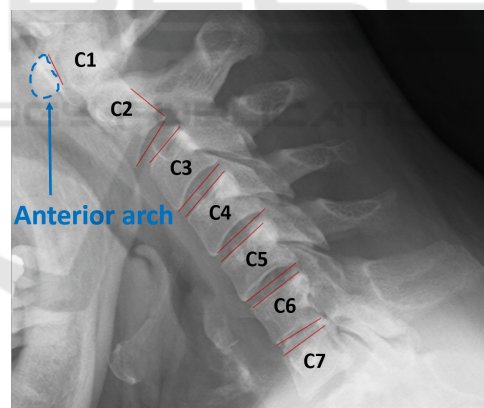


Figure 1: Example of annotation for measurement.

When the neck is moved, movement occurs in each of the C1–C7 vertebra (Figure 1). In specific regard to flexion and extension, cervical instability may be assessed by analyzing the mobility between vertebrae from cervical X-ray images. For this evaluation, it is necessary to measure each range of motion (RoM) angle between C1 and C7. In the Bakke method, which is one of the measurements performed by the physician, X-ray images are taken when the cervical region is flexed and extended, and lines are drawn at the upper and lower edges between each vertebra. The next step is to find the angle between

<sup>a</sup> <https://orcid.org/0000-0001-9753-2983>

<sup>b</sup> <https://orcid.org/0000-0003-3733-0188>

<sup>c</sup> <https://orcid.org/0000-0002-1676-7578>

<sup>d</sup> <https://orcid.org/0000-0002-5993-2297>

<sup>e</sup> <https://orcid.org/0000-0003-3735-4809>

these lines and take the difference between the angle for flexion and the angle for extension. Due to the special shape of C1 and C2, a line is drawn on the posterior margin of the anterior arch for C1 and on the posterior margin of the vertebral body for C2, and the angle between these lines is determined (Figure 1). In this method, a total of 24 lines are drawn on the cervical spine images of flexion and extension, which creates a significant burden for the physician who has to check them. Moreover, the C1 and C2 vertebrae are particularly difficult to measure accurately because of their special shape. In this study, we aim to support physicians in measuring the RoM angles by implementing a system that automates the measurement of RoM angles from cervical spine X-ray images.

## 2 RELATED WORK

### 2.1 Medical Image Segmentation

Segmentation using image processing has been studied. Huaifei et al. proposed a method using image processing to extract a rough cervical spine region by contrast histogram and then estimate the region by using curve fitting (Huaifei et al., 2011). In addition, Lecron et al. proposed a method to detect the corners of each cervical spine section by using edge detection and Hough transform for segmentation (Lecron et al., 2010). Segmentation using such image processing techniques requires a large number of parameters to be set and threshold values to be determined, which makes the implementation more complex. Moreover, in order to avoid the influence of the head when focusing on the histogram, it is necessary to crop only the cervical region from the original X-ray image.

Recently, segmentation methods based on deep learning have been proposed. Architectures used for such segmentation include Fully Convolutional Networks (FCN) (Long et al., 2015), U-Net (Ronneberger et al., 2015), and Mask R-CNN (He et al., 2017). Arif et al. proposed an FCN-based Convolutional Neural Network (CNN) called SPNet for cervical spine segmentation (Arif et al., 2018) that, compared with existing methods such as U-Net, can robustly detect the cervical region even in images contaminated with foreign matter. Masuzawa et al. proposed a method for automatic segmentation, localization, and identification of vertebrae in arbitrary 3D CT images. They developed a network for instance segmentation of cervical, thoracic, and lumbar vertebrae from 3D CT images (Masuzawa et al., 2020). Uozumi et al. used Mask R-CNN to extract lung regions from chest X-ray images with high accuracy (Uozumi et al.,

2020) and found that, while U-Net is more accurate in terms of extraction accuracy, Mask R-CNN is more robust to the diversity caused by changes in the shading of X-ray images and changes in the position of the lungs due to disease. Mask R-CNN has the advantage of being able to process each cervical spine section separately since, unlike other networks specialized for segmentation, it performs instance segmentation. In the present work, we extract the cervical spine region from the cervical spine X-ray image by using Mask R-CNN. The contribution of our research is that we did a segmentation of the cervical spine and then measured the RoM of the cervical spine and evaluated the accuracy of the measurement with the physician.

### 2.2 Computer Aided Diagnosis for Cervical Spine

Various research is being conducted to analyze and diagnose medical images using segmentation techniques, image processing, and deep learning to assist physicians in diagnosis. Choi et al. developed a system to estimate the spinal column alignment from moiré images by training a set of moiré images and lumbar spine X-ray images using CNN and then measuring the Cobb angle, which represents the degree of the curve of the spine (Choi et al., 2017). The average error from the true value in their system was 3.8 degrees, which is equivalent to the accuracy of measurement by a physician. Alomari et al. developed a system to segment lumbar discs by using image intensity and gradient vector flux and to detect disc abnormalities by measuring the disc height (Alomari et al., 2011). Young et al. used deep learning and image processing to measure the thickness of the prevertebral soft tissue in front of the vertebral body from cervical spine X-ray images, and proposed a method to diagnose swelling by referring to the flow of swelling diagnosis by physicians (Young et al., 2018).

In the present study, we measure the RoM angle between sections of the cervical spine by using a system implemented with reference to the diagnostic flow of a physician. By measuring this RoM, the features of the cervical vertebrae are detected and used to help the physician make a diagnosis. The computer-based measurement is expected to have the advantage of eliminating the variation in measurement among physicians.

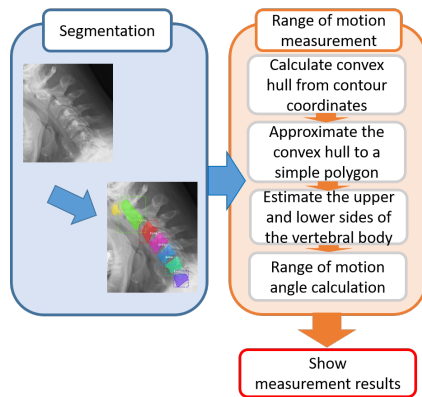


Figure 2: System flow.

### 3 METHOD

#### 3.1 Overview of System

The flow of the system proposed in this study is shown in Figure 2. First, the cervical spine region is estimated from the cervical spine X-ray image using Mask R-CNN. The estimated region is approximated by a simple polygon with three or four vertices. The edges of the polygons of cervical spine  $n$  and cervical spine  $n+1$ , which are close to the center of each other, are the edges that lie between the cervical spine vertebrae. The RoM angle is calculated by measuring the angle between the cervical spine in the flexion image and the extension image, and then calculating the difference.

#### 3.2 Estimation of Cervical Spine Region

The training data are X-ray images of the cervical spine when it is flexed and extended. Based on the guidance of a radiologist specializing in the cervical spine, cervical spine mask information is created, and the pair with the original image is used as training data. The cervical spine regions to be masked are different for C3 to C7 and for C1 and C2 because of the special shape of the latter. Specifically, the C1 region is the anterior arch, and the C2 region includes the entire vertebrae from the vertebral body to the odontoid process. The regions are labeled as c1, c2, and bone (Figure 3).

#### 3.3 RoM Angle Measurement from Estimated Cervical Region

The bounding box coordinates and area information of the regions estimated by Mask R-CNN are stored

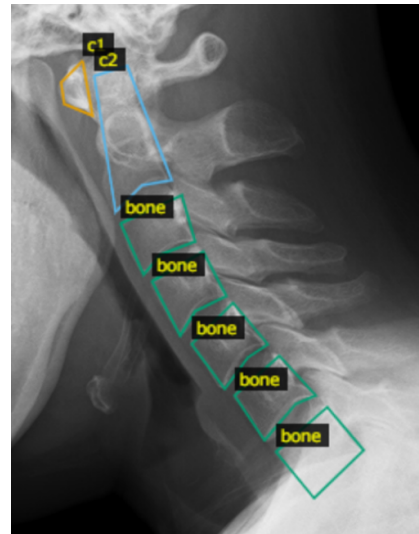


Figure 3: Annotation area.

in an array, but they are not arranged in the order of C1 to C7. Therefore, it is necessary to shift the cervical spine positions of the estimated regions in both images so that they correspond. To prepare for the measurement, the y-coordinates of the bounding box should be in ascending order, and the estimated regions should be rearranged in the order of C1 to C7. However, it is sometimes not possible to estimate some of the cervical regions in the image. In such cases, we take the difference between the y-coordinates of the upper left and lower right of the rectangle of cervical spine  $n$  and cervical spine  $n+1$ , and consider it continuous if it is less than half of the height of the bounding box of cervical spine  $n$ . If this condition is not met, it is judged that there is a mis-estimated region or a cervical region that cannot be estimated. The flow of the automatic annotation is shown in Figure 4. First, the contour coordinates of the region are obtained from the estimated cervical region (Figure 4(a)). The coordinates of the convex hull are selected from the contour coordinates and then the convex hull region is approximated as a polygon with three or four vertices (Figure 4(b), (c)). After this, the midpoint of each edge of the approximated polygon is calculated. The edge where the calculated midpoints are close to each other (between cervical spine  $n$  and cervical spine  $n+1$ ) is regarded as the edge of the cervical spine used for measurement (Figure 4(d)). However, since approximate polygons below C3 are approximated to be inscribed in the convex hull region, their edges may be far from the contour coordinates of the estimated region. In this case, we extract the contour coordinates near the selected edge in the approximate polygon (Figure 4(f)). Let  $x_1$  and  $y_1$  be the coordinates of the left end of the selected edge in

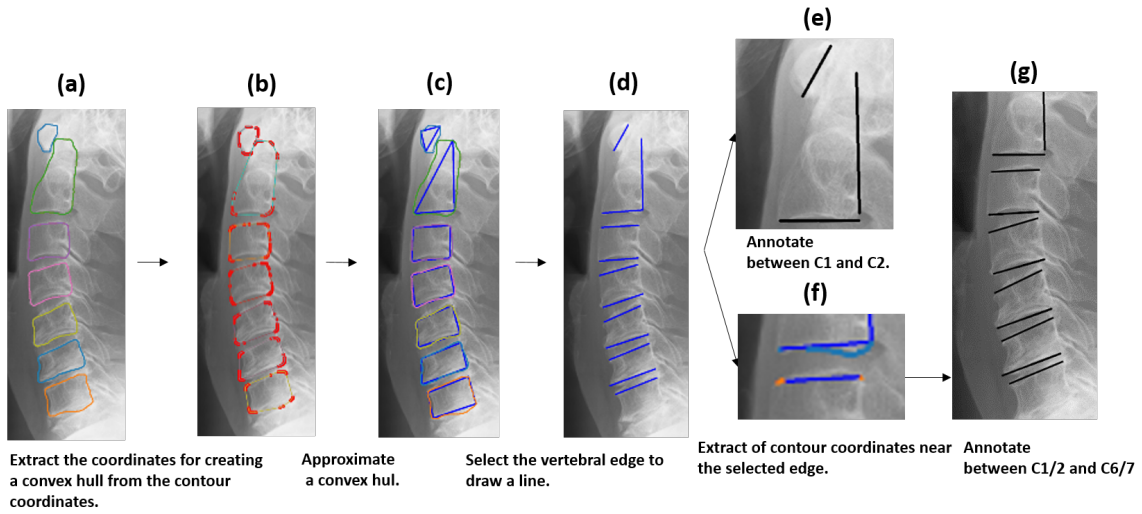


Figure 4: Flow of automatic annotation.

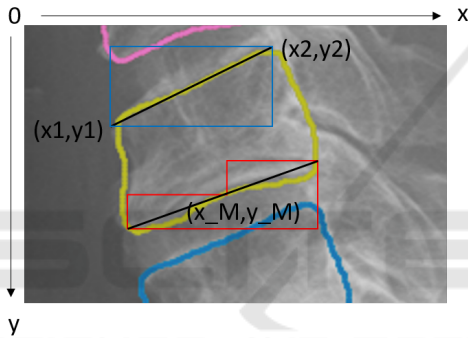


Figure 5: Extraction range of coordinates through which the line passes.

the approximate polygon,  $x_2$  and  $y_2$  be the right ends, and  $x_M$  and  $y_M$  be the midpoints (Figure 5). If we denote the  $x$ -coordinate group of the contour coordinates as  $verts\_x$  and the  $y$ -coordinate group as  $verts\_y$ , the upper edge of the vertebra of interest is the contour coordinate that satisfies the conditions of Equation 1, and is the contour coordinate in the blue box in Figure 5. The lower edge is the contour coordinate that satisfies the conditions of Equation 2, which is the contour coordinate in the red box in Figure 5. A line is drawn on these coordinates using the least-squares method to find the angle between them (Figure 4(g)). The angle between the two lines is calculated from Tangent's additive theorem by using Equation 3, where  $a$  and  $b$  are the slopes of the two lines.

$$(x_1 \leq verts\_x \leq x_2) \cap (y_2 \leq verts\_y \leq y_1) \quad (1)$$

$$\begin{cases} (x_1 \leq verts\_x \leq x_M) \cap (y_M \leq verts\_y \leq y_1) \\ (x_M \leq verts\_x \leq x_2) \cap (y_2 \leq verts\_y) \end{cases} \quad (2)$$

$$\tan\Theta = \frac{a-b}{1+ab} \quad (3)$$

## 4 EVALUATION

### 4.1 Conditions for Learning Model of Cervical Spine Region

The dataset used in this study consisted of 968 X-ray images of cervical spine flexion and extension in 484 individuals aged between 20 and 100 years who were patients at the Department of Radiology, Tokyo Medical and Dental University Medical Hospital. Of these 968 images, 922 (461 patients) were used as training data, and the remaining 46 (23 patients) were used as test data.

We used the weights learned by Microsoft COCO as the initial weights and updated them by re-training the entire network with the created training data. The training parameters are listed in Table 1. The 922 training data were divided so that the ratio of training data to validation data was 8 to 2. The learning parameters in this experiment were as follows.

### 4.2 Results and Discussion of Learning Model for Cervical Region

We performed estimation on 46 images of the test data. Out of a total of 322 cervical vertebrae in these 46 images, 313 were successfully estimated. This means that 97% of the total test data was able to be detected. Intersection over Union (IoU), which is the similarity between two sets, was used to evaluate the

Table 1: Hyperparameters.

Training data	756 images
Validation data	166 images
Classification	Three-class classification
Number of epochs	100
Image size	$512 \times 512$ px
Batch size	1
Learning coefficient	0.001
Optimization method	Stochastic gradient descent

Table 2: IoU of each cervical spine.

Position	IoU
C1	0.74
C2	0.83
C3	0.88
C4	0.88
C5	0.87
C6	0.86
C7	0.86
Average	0.85

estimated cervical region. The IoU value is obtained by dividing the common part of the correct and estimated regions by the union of the two regions, where the maximum value is represented by 1. The higher the value, the higher the accuracy of the object detection. The IoU values for each cervical spine vertebra are shown in Table 2. The mean IoU value for all 46 test data was 0.85.

### 4.3 Accuracy Comparison between Proposed System Measurements and Resident Measurements

The measurement accuracy of the automatic measurement method was evaluated by comparing the average error between the true value and the automatic measurement value, and between the true value and the resident's measurement value, using the specialist's measurement as the true value. A specialist in this context refers to a physician who specializes in the diagnosis of the cervical spine, while a resident refers to a physician who does not specialize in the diagnosis of the cervical spine.

The data to be measured were the same 46 images of the test data (23 patients) used to validate the learning model in the cervical region. The true value was measured 69 times by two specialists, 23 persons (test data)  $\times$  3 times (number of measurements). The frequency of measurement was limited to once a day

and was not continuous. The true value is the average of the three measurements taken by two medical specialists. Two residents who were given guidance on the cervical RoM angle measurement by a specialist were asked to measure the test data under the same conditions as the specialist. In the measurement of the RoM angle in the test data, the number of places where automatic measurement was possible was 133 out of 138 places for 23 persons  $\times$  6 (places where the RoM angle was measured). The remaining five places were not measured because the cervical region could not be estimated: the cervical regions were not segmented at all.

The error between the true value and the automatic measurement value was calculated by averaging the difference between the two for each vertebra as an absolute value. The error between the true value and the value measured by a resident was calculated by averaging the difference between the true value and the resident's measurement between each cervical spine for each of the three times the resident performed the measurement. The mean error between the true value of the RoM angle between each vertebra in the automatic and resident measurements is shown in Table 3. We also calculated the standard deviations for each measurement by the specialist and the residents, with the results shown in Table 4. In the automatic measurement, the standard deviation was 0 because the same value was obtained even after three measurements.

We compared the errors of the true value and the automatic measurement with those of the true value and the residents measurement. Figure 6 shows the comparison of the average error between the resident and automatic measurements. There was no difference in the overall mean error between the automatic and residents measurement. However, the variance in error was smaller for the automatic measurement. We performed a two-sided t-test at the 5% level of significance to see if these was statistically significant. Variable 1 is the error value of the resident, and the number of samples was 798: resident (2 persons)  $\times$  number of measurements (3 times)  $\times$  133/138 cervical intervals. Variable 2 is the error value of the automatic measurement, and the number of samples was 798: 133/138 cervical spine  $\times$  the number of measurements of the system (6 times). There was no significant difference in the average error between the resident and automatic measurements. We examined the significant differences in the errors for each of C1/2–C6/7. There is a significant difference in C2/3 and C5/6 and the resident has a smaller error. C3/4 and C4/5 have also significant but the automatic measurement has a smaller error.

Table 3: Average error compared to the specialist measurement.

vertebrae	Automatic measurement (deg)		Resident measurement (deg)	
	Average error	Standard deviation	Average error	Standard deviation
C1/2	5.7	4.4	5.9	8.9
C2/3	4.0	3.6	2.9	2.3
C3/4	2.5	2.4	3.1	2.7
C4/5	2.6	2.1	3.3	2.7
C5/6	3.6	2.3	2.8	2.2
C6/7	2.5	2.2	2.6	1.9
Average	3.5	2.8	3.5	3.4

Table 4: Standard deviation of specialist and resident measurements.

Vertebra	Specialist value (deg)	Resident value (deg)
	Standard deviation	Standard deviation
C1/2	4.4	5.2
C2/3	2.4	2.6
C3/4	2.9	2.9
C4/5	2.5	3.0
C5/6	2.7	2.7
C6/7	2.4	2.7
Average	2.9	3.2

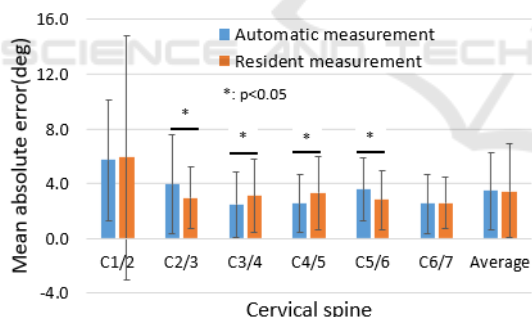


Figure 6: Comparison of mean error between resident measurements and automatic measurements.

### 4.4 Discussion

Figure 7 shows an example of the correct estimation of C1 to C7, where the green color represents the correct region and the red color represents the estimated region. The average IoU in this case was over 0.85. Examples of incorrect estimation are shown in Figure 8. Cases (a), (c), and (d) were presumably caused by a lack of training data, while case (b) seems to have stemmed from a problem with the X-ray image. In the future, we discuss whether it is possible to measure the RoM angle of the part that could not be measured

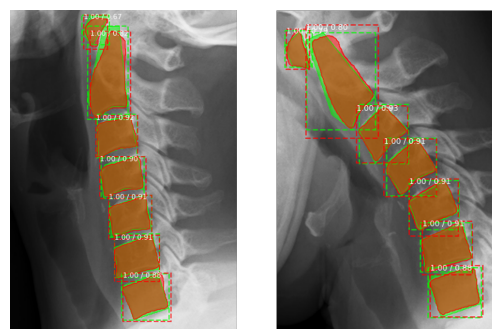


Figure 7: Example of correct estimation.

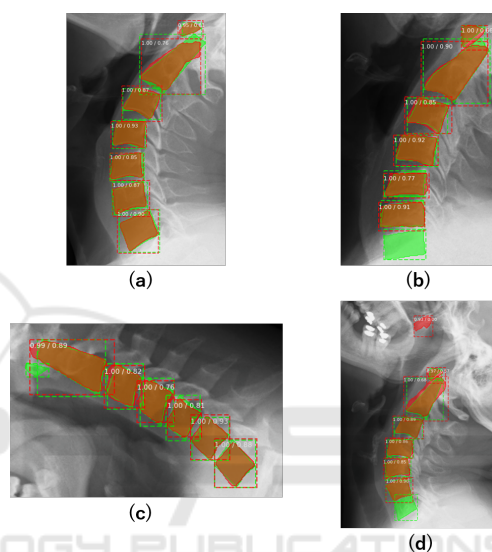


Figure 8: Examples of incorrect estimation: (a) Large missing estimation area. (b) C6 and C7 are hidden in the patient's chest and cannot be estimated. (c) C1 is not estimable. (d) Non-cervical region estimated to be cervical spine.

by our method by learning the past RoM angle values measured by physicians and images as a set and then performing regression analysis.

According to the results in 4.2, the IoU values of C1 were smaller than those of other cervical regions. The IoU values of C2 also tended to be smaller than those of C3 to C7. This indicates that the estimation accuracy of the cervical region of C1 and C2 is low. Moreover, the accuracy of the proposed system was particularly poor for C1/2 between C1/2 and C6/7. One of the factors that reduced the measurement accuracy was the low estimation accuracy of the cervical region of C1 and C2. The reason for this low estimation accuracy is that C1 and C2 are labeled differently, and there is only one region in one image, but C3 through C7 are labeled the same, so there are four regions in one image. We therefore conclude that the IoU values of C1 and C2 were lower be-

cause these two vertebrae had less training data than C3–C7. However, although the IoU value tends to increase as the number of training images is increased, the IoU values of C2–C7 at the current number of images tends to reach a peak. As for C1, the trend of increasing IoU value is seen. From the above, the current number of data sets is sufficient for C2–C7. On the other hand, it is expected that even if the number of training images is increased, the IoU only increases for C1. If we can increase the amount of training data, we should be able to improve the accuracy of the estimation of C1.

## 5 CONCLUSION

In this paper, we proposed a cervical spine RoM angle measurement assistance system to measure the cervical RoM angle by using image analysis. Our findings showed that Mask R-CNN estimation of the cervical region was able to estimate 97% of the total test data, resulting in an overall IoU of 0.85. The standard deviation of the measurements was 2.9 degrees among the specialists and 3.2 degrees among the residents, while that of the proposed system was just 0, as the measurements did not change no matter how many times they were taken. The reproducibility, which is an advantage of computer vision technology, allowed the physician's measurements to overcome the problem of inconsistent values. The mean measurement error of the proposed system and residents were same value: 3.5 degrees. In the errors for each of C1/2–C6/7, there is a significant difference in C2/3, C3/4, C4/5, and C5/6. However, there was no significant difference in the overall mean error between the automatic measurement and the resident's measurement.

In the analysis of cervical X-ray images, attention should be paid not only to the RoM angle but also to the normal alignment of the cervical spine. In future work, we will increase the amount of training data to improve the accuracy of cervical spine region estimation and see if we can determine the cervical misalignment to estimate the defective cervical spine region. We also plan to try other segmentation methods to compare the accuracy of the cervical region estimation and the accuracy of the RoM measurement.

## ACKNOWLEDGEMENTS

This work was supported by JST AIP-PRISM, grant number JPMJCR18Y2; and JSPS KAKENHI, grant number JP21H03485. We appreciate Dr. Kaburaki

of Tokyo Medical and Dental University for his cooperation in the measurements and Assistant Professor Ienaga for his advice on this study.

## REFERENCES

- Alomari, R., Chaudhary, V., and Dhillon, G. (2011). Computer aided diagnosis system for lumbar spine. In *Proceedings of the 4th International Symposium on Applied Sciences in Biomedical and Communication Technologies*, pages 1–5. ACM.
- Arif, S. A., Knapp, K., and Slabaugh, G. (2018). Spnet: shape prediction using a fully convolutional neural network. In *International Conference on Medical Image Computing and Computer-Assisted Intervention*, page 430–439.
- Choi, R., Watanabe, K., Jinguji, H., Fujita, N., Ogura, Y., Demura, S., Kotani, T., Wada, K., Miyazaki, M., Shigematsu, H., and Aoi, Y. (2017). Cnn-based spine and cobb angle estimator using moire images. *IEEE Transactions on Image Electronics and Visual Computing*, 5(2):135–144.
- He, K., Gkioxari, G., Dollar, P., and Girshick, R. (2017). Mask r-cnn. In *Proceedings of the IEEE International Conference on Computer Vision*, page 2961–2969.
- Huaifei, H., Liu, H., Chen, L., and Hung, C. (2011). Image segmentation of cervical vertebra in x-ray radiographs using the curve fitting strategy. In *Proceedings of the 2011 ACM Symposium on Applied Computing*, page 853–858.
- Lecron, F., Benjelloun, M., and Mahmoudi, S. (2010). Points of interest detection in cervical spine radiographs by polygonal approximation. In *International Conference on Image Processing Theory*. IEEE.
- Long, J., Shelhamer, E., and Darrell, T. (2015). Fully convolutional networks for semantic segmentation. In *Proceedings of the IEEE Conference on Computer Vision and Pattern Recognition*, page 3431–3440. IEEE.
- Masuzawa, N., Kitamura, Y., Nakamura, K., Iizuka, S., and Simo-Serra, E. (2020). Automatic segmentation, localization, and identification of vertebrae in 3d ct images using cascaded convolutional neural networks. In *Medical Image Computing and Computer Assisted Intervention – MICCAI 2020*, page 681–690.
- Ronneberger, O., Fischer, P., and Brox, T. (2015). U-net: Convolutional networks for biomedical image segmentation. In *International Conference on Medical Image Computing and Computer-Assisted Intervention*, page 234–241.
- Uozumi, H., Matsubara, N., Teramoto, A., Niki, A., Honmoto, T., Kono, T., Saito, K., and Fujita, H. (2020). Lung region segmentation on pediatric chest x-rays using mask r-cnn in japanese. *Med Imag Tech*, 38(3):126–131.
- Young, H., Sewon, K., Suh, J., and Hwang, D. (2018). Learning radiologist's step-by-step skill for cervical spinal injury examination: Line drawing, prevertebral soft tissue thickness measurement, and swelling detection. volume 6, pages 55492–55500.